

Incommensurate icosahedral density waves in rapidly cooled metals

David R. Nelson and Subir Sachdev

Department of Physics, Harvard University, Cambridge, Massachusetts 02138

(Received 8 February 1985)

There are three simple phenomenological descriptions of incommensurate icosahedral density waves in rapidly cooled metals, based on stars of the reciprocal-lattice vectors which point to the vertices, edges, or faces of an icosahedron. The icosahedral phase of $\text{Al}_{0.86}\text{Mn}_{0.14}$ is described by the vertex model. We also discuss extended icosahedral correlations present in a hierarchical Frank-Kasper phase proposed by Mosseri and Sadoc.

I. LANDAU THEORY AND $\text{Al}_{0.86}\text{Mn}_{0.14}$

Recently Shechtman *et al.*¹ have reported the discovery of a phase of $\text{Al}_{0.86}\text{Mn}_{0.14}$ with well-defined diffraction spots obeying an icosahedral point group symmetry. Their observations are consistent with long-range icosahedral order, with a range of at least $1\ \mu\text{m}$. Two models of long-range icosahedral order are possible. One, proposed by Steinhardt *et al.*,² posits long-range order in the orientations of icosahedral packing units, with a finite (but possibly large) translational correlation length, similar to the bulk hexatic phase of smectic-*B* liquid crystals.³ In liquid crystals, one observes a pattern of intensity maxima in the in-plane scattering characteristic of a two-dimensional hexagonal close-packed lattice. The translational correlation length, however, as measured by the inverse radial width of the Bragg spots, is finite. In the hexatic-*B* phase of 95SBC (*n*-nonyl 4'-*n*-pentylbiphenyl-4-thiocarboxylate), for example, this length can be as large as $500\ \text{\AA}$ —about 100 molecular diameters.³

The second model postulates a superposition of density waves with an icosahedral symmetry, leading to a state with long-range orientational *and* translational order. Here the Bragg peaks would be true delta functions, with additional $1/q^2$ tails if thermal fluctuations are important. Levine and Steinhardt⁴ have proposed a specific Penrose pattern⁵ to model $\text{Al}_{0.86}\text{Mn}_{0.14}$, and show that a simplified version of this model leads to an icosahedrally symmetric pattern of delta-function Bragg-peaks in reciprocal space. Even if the translational correlation length in $\text{Al}_{0.86}\text{Mn}_{0.14}$ turns out to be finite, icosahedral density-wave models may provide a good indication of the experimentally observed peak positions. Levine and Steinhardt find good agreement with the experimentally observed diffraction peaks patterns in planes through the origin and normal to the fivefold and threefold icosahedral symmetry axes. (The agreement normal to the twofold axis was not as good, however, for the simplified model.) The precise connection between the positions of aluminum and manganese atoms and the rhombahedral “bricks” which give rise to a Penrose pattern is, at present, unclear.

Icosahedral density waves can also be described using a purely phenomenological approach due to Landau.⁶ One starts by expanding the particle density in an isotropic liquid in the plane waves whose amplitudes become large

in the ordered phase:

$$\rho(\mathbf{r}) = \rho_0 + \sum_{\mathbf{G}} \rho_{\mathbf{G}} e^{i\mathbf{G}\cdot\mathbf{r}}. \quad (1)$$

For simplicity, we restrict our attention to \mathbf{G} 's whose magnitudes match the position of the first peak in the liquid-structure factor. The free-energy density is constructed as an expansion in rotationally and translationally invariant combinations of the expansion coefficients $\rho_{\mathbf{G}}$.

$$\mathcal{F} = \frac{1}{2} r \sum_{\mathbf{G}} |\rho_{\mathbf{G}}|^2 + w \sum_{\mathbf{G}_1 + \mathbf{G}_2 + \mathbf{G}_3 = 0} \rho_{\mathbf{G}_1} \rho_{\mathbf{G}_2} \rho_{\mathbf{G}_3} + \dots \quad (2)$$

At low temperatures, the coefficient of the quadratic term is assumed to be negative, and the ordered phase is constructed from a “star” of wave vectors lying on a sphere of radius G in reciprocal space. The third-order term ensures that the transition is first order. The particular subset of reciprocal-lattice vectors which order is determined by the combined effect of all such nonlinearities in (2). Other nonlinear terms in this expansion ensure that ordering also occurs at “harmonics” given by all possible linear combinations of the fundamental star.

Particularly simple lattices are associated with stars with a high degree of symmetry. The simple cubic, fcc, and bcc lattices, for example, are generated by stars which point, respectively, to the vertices, faces, and edges of a regular octahedron. In view of the results of Shechtman *et al.*,¹ it is natural to consider stars composed of reciprocal-lattice vectors pointing to either the 12 vertices, 30 edges, or 20 faces of a regular icosahedron. Alexander and McTague⁷ used the edge model to describe short-range icosahedral order in liquids. They went on to argue, along lines taken earlier by Baym *et al.*,⁶ that the edge model would be preferred in the limit of an infinitely weak first-order transition. Freezing transitions are usually strongly first order, however, and, as we show below, the icosahedral phase of Al-Mn is in fact best described by the *vertex* model.

Phases described by icosahedral stars are fascinating, because the basis vectors comprising the stars are incommensurate. Instead of a regular lattice of intensity maxima in reciprocal space, one can generate peaks *arbitrarily* close to any given position by taking increasing complex linear combinations of the fundamental basis set. Within Landau theory, one expects a decreasing hierarchy of peak

intensities, depending on how many elements of the star were required to make a particular peak. The two-dimensional Penrose patterns⁵ have a structure factor characterized by a symmetrical ten-element incommensurate star of reciprocal-lattice vectors pointing to the vertices of a regular decagon. Its existence is closely related to the concept of "pentagrids" introduced by de Bruijn.⁸

Landau theory suggests that the bewildering pattern of peaks observed experimentally in Al-Mn can be indexed to one simple basis set. We shall refer to peaks as belonging to the n th Landau generation if the minimum number of elements in the star required to produce them is n . Only the edge model leads to a tenfold spot pattern normal to a fivefold symmetry axis, and a sixfold spot pattern normal to a threefold axis in the first generation. One cannot use this criterion to distinguish the edge model, however, because spots with the same symmetry appear in the vertex and face models already in the second generation. Indeed, one can show that the spot positions normal to the fivefold and threefold axes are identical, up to a change of scale in the edge, vertex, and face models. As shown in Fig. 1, a clear distinction between the various models emerges only when one looks at spots normal to the twofold axis. Four generations of spots are shown; the vertex, edge, and face models each have four primary spots in this plane, forming, respectively, a golden rectangle, a square, and a more elongated rectangle. The spots in the edge model are a subset of the spots in the vertex and face models. It can be shown that the spot *positions* in the vertex and face models can be made to coincide. The hierarchy of intensities predicted by Landau theory, however, is qualitatively different. A glance at the data of Shechtman *et al.*¹ strongly suggests that the vertex model provides the best fit. A more detailed comparison is shown in Fig. 2, where seven generations of vertex model spots are compared to transmission electron microscope diffraction data of Kelton and Wu.⁹ Both the peak positions and the sequence of diminishing intensities are properly accounted for. The agreement is equally good for the threefold and fivefold axes. The first generation spots occur at a position comparable to the expected location of the first peak in the structure factor of liquid Al-Mn. It is remarkable that the complex of experimentally observed spots in $\text{Al}_{0.86}\text{Mn}_{0.14}$ can be indexed to a basis set of just 12 vectors.

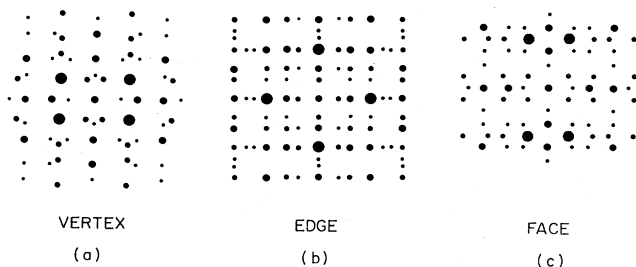


FIG. 1. Patterns of diffraction spots in reciprocal space plane through the origin and normal to the twofold symmetry axis of an icosahedron for the vertex, edge, and face models. Four generations of spots are shown; larger spots correspond to earlier generations.

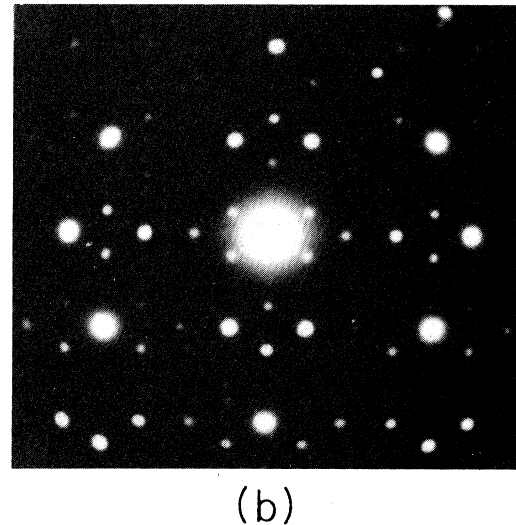
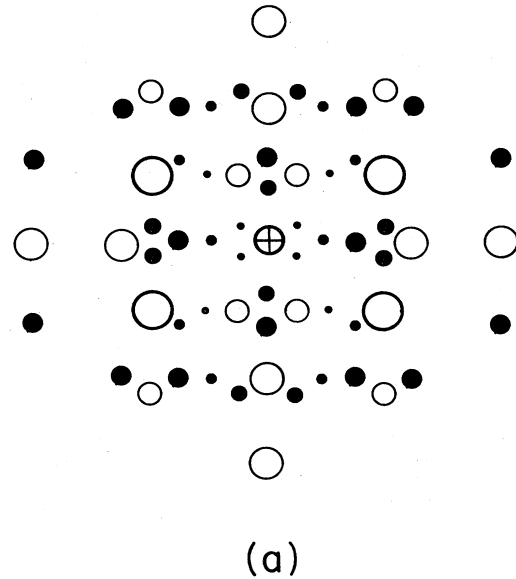


FIG. 2. (a) First seven generations of spots normal to the twofold axis for the vertex model. (b) Experimental twofold diffraction pattern for $\text{Al}_{0.86}\text{Mn}_{0.14}$ (Ref. 9).

Just as in charge-density-wave incommensurate systems, this hierarchy of spots suggests a hierarchy of gaps in the band structure of these materials.⁴ One simple argument proceeds as follows: in a nearly free-electron model, the potential $V(\mathbf{r})$ seen by an electron will have a large Fourier component V_G whenever G is a member of the icosahedral reciprocal lattice discussed above. Standard methods¹⁰ then lead to a gap in the free-electron spectrum $E(\mathbf{k}) = \hbar^2 k^2 / 2m$ of order $|V_G|$ at wave vectors \mathbf{k} such that

$$\mathbf{k} \cdot \mathbf{G} = \frac{1}{2} G^2. \quad (3)$$

II. A FRANK-KASPER PHASE WITH EXTENDED ICOSAHEDRAL ORDER

The discussion in the preceding section is phenomenological, and does not address the question of particle posi-

tions in real space. The most striking characteristic of the Penrose patterns is the long-range orientational order of the Penrose bricks in real space. Here, we now show that there are also extended icosahedral correlations in a hierarchical Frank-Kasper phase proposed by Mosseri and Sadoc.¹¹ The model was originally conceived as a way of flattening an ideal icosahedral crystal (called polytope $\{3,3,5\}$) imbedded in the curved surface of a four-dimensional sphere. The flattening is achieved by introducing successive generations of -72° -wedge disclination lines according to certain rules. Locally, the particles form slightly distorted tetrahedra, which combine to form icosahedra, threaded by the disclination network. The Frank-Kasper phases¹² of transition-metal alloys can also be regarded in this way,¹³ except that the disclinations arrays exhibit conventional crystalline periodicities. These special particle configurations play an important role in recent theories of metallic glasses. Mosseri and Sadoc point out that the limiting structure is likely to be "more ordered" than a metallic glass. Here, we carry out the construction directly in flat space, and show that the structure factor has long-range orientational order, despite the presence of a dense network of disclination lines.

To motivate our adaptation of the Mosseri-Sadoc model to flat space, consider first the problem of densely packing the plane with identical particles. The natural packing unit is an equilateral triangle, and we use six such triangles to form a perfect hexagon composed of seven particles. As shown in Fig. 3(a), each bond of every triangle is then divided into thirds by adding two additional particles. Yet another particle is inserted at the center of each triangle. By drawing near-neighbor bonds between both old and new particles, one obtains nine new smaller triangles. Iterating this process, and appropriately scaling up the particle size, one trivially obtains a hexagonal close-packed lattice.

This construction is nontrivial when applied to three dimensions, where frustration prevents packings composed only of perfect tetrahedra.¹³ We start by combining 20 tetrahedra to form a regular icosahedron of 13 particles. The tetrahedra formed by clusters of four neighboring particles are slightly distorted, with the bonds at the surface about 5% longer than the bonds to the center. The generalization of the two-dimensional construction is shown in Fig. 3(b). One new particle is placed at the center of mass of each tetrahedron, and each bond is again divided into thirds by the addition of two more new particles. Just as in $d=2$, all the old particles are retained. When near neighbors are assigned using the Voronoi construction, four pairs of smaller tetrahedra appear at the vertices of each original tetrahedron. The Voronoi construction also leads to near-neighbor bonds between the particles placed at the centers of neighboring large tetrahedra, with one such bond exiting through each of the four faces of every tetrahedron. There are six small tetrahedra wrapped around every such bond; these are shared between the two large tetrahedra linked by the bond. Thus, in all, $4 \times 2 + 4 \times \frac{6}{2} = 20$ smaller tetrahedra are generated for each large one. These tetrahedra are slightly distorted, even if the initial tetrahedron is perfect.

This operation can be repeated on each of the new

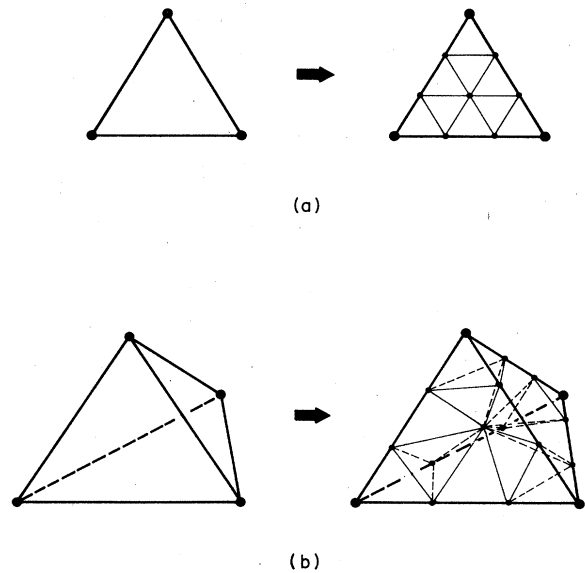


FIG. 3. Iterative procedures for generating close packings of (a) triangles in two dimensions and (b) tetrahedra in three dimensions.

tetrahedra. Many such iterations, each followed by a length rescaling, leads to an infinite lattice of distorted tetrahedra. One might think that the distortions in the tetrahedra might build up with iteration. This has not happened in our numerical studies of high-order iterates, and, indeed, should not be expected because one is in fact constructing a kind of Frank-Kasper phase.¹² Many particles sit in icosahedral coordination shells. This icosahedral order, however, is interrupted by a network of -72° -wedge disclination lines.¹³ Three typical coordination shells, called Z12, Z14, and Z16, are shown in Fig. 4. All bonds from the central atom to the icosahedral shell Z12 have five tetrahedra wrapped around them, and are defined to be defect free. As shown in the figure, two of the 14 atoms in Z14 are associated with sixfold bonds, which are colinear links of disclination line. Four out of the 16 atoms in Z16 terminate a set of four disclination links meeting at the central atom. All remaining bonds to the central atom in Z14 and Z16 are fivefold. In the Frank-Kasper phases, the wedge disclination links associated with Z14, Z16 (and another coordination shell called Z15) occur in just the right proportions to ensure minimally distorted tetrahedra.^{12,13} This is also true of the Mosseri-Sadoc model.¹¹

Mosseri and Sadoc show that their curved space construction leads to only Z12, Z14, and Z16 coordination sites. They derive a recursion relation for the number of new Z12's, Z14's, and Z16's, namely

$$\begin{pmatrix} Z12' \\ Z14' \\ Z16' \end{pmatrix} = \begin{pmatrix} 13 & 12 & 12 \\ 0 & 3 & 4 \\ 5 & 6 & 8 \end{pmatrix} \begin{pmatrix} Z12 \\ Z14 \\ Z16 \end{pmatrix}. \quad (4)$$

The derivation is topological, and does not really depend on whether the construction is carried out in curved or flat space. To illustrate their argument, consider what

happens when the transformation of Fig. 3(b) is applied to the 28 tetrahedra comprising a Z16 coordination shell. The Z16 at the center remains a Z16. Our earlier discussion of Fig. 3(b) makes it clear that 28 new Z16's are generated at the centers of each of the 28 tetrahedra. These must be shared between four old vertices, however, for a total of seven per vertex. Each old Z16 vertex, of course, remains a Z16. It remains to determine the coordination topology of the new particles one-third of the way out on the 16 bonds radiating from the center. There are 12 five-fold bonds. Each one of these is surrounded by an icosahedral shell with its north pole two-thirds of the way along the bond and its south pole at the center of the initial Z16. This Z12 coordination shell is completed by two staggered pentagonal rings. The one nearest the north pole comes from the particles at the centers of the five tetrahedra surrounding the bond; the ring nearest the south pole comes from the particles one-third of the way along the five bonds which surround the bond in question. Thus, each Z16 generates 12 new Z12's. In a very similar way, the four sixfold bonds give rise to four new Z14's. In summary then, we have shown that

$$\text{Z16} \rightarrow 12(\text{Z12}) + 4(\text{Z14}) + 8(\text{Z16}), \quad (5)$$

which accounts for the last column in Eq. (4).

The asymptotic distribution of coordination shells is given by the largest eigenvector of Eq. (4).¹¹ It follows that the limiting fractions of Z12's, Z14's, and Z16's are 36/57, 4/57, and 17/57, respectively. The predominantly icosahedral sites in this structure are laced with a hierarchical network of disclination lines. Applying the construction to a regular icosahedron, for example, gives disclination links along the edges of a regular dodecahedron, similar to the network in the Frank-Kasper phase $\text{Mg}_{32}(\text{AlZn})_{49}$.¹² An additional disclination network threads the tetrahedra in this new structure after the next iteration, and so on. The construction preserves the disclination networks present in all previous generations. Although the limiting particle configuration is aperiodic,¹¹ the local coordination topologies are indistinguishable from those in a conventional Frank-Kasper phase.

We have studied correlations in the Mosseri-Sadoc model by applying the construction several times, starting with the 20 tetrahedra in a regular icosahedron, and then Fourier transforming the resulting particle configuration. The particles were relaxed (via a conjugate gradient technique) in a Lennard-Jones pair potential. We first minimized with respect to dilations to determine a position for the minimum in the potential, and then allowed an unconstrained relaxation. The large particle clusters obtained in this way are somewhat similar to the icosahedral "amorphons" discussed by Hoare.¹⁴ Unlike most large "amorphons," however, they contain no octahedral configurations, either before or after relaxation. They can, moreover, be made arbitrarily large by repeated iterations. There is a kind of translational invariance, in the sense that all new icosahedra generated after a given iteration are subsequently treated in the same way as the initial icosahedral seed. This self-similarity is also a property of the Penrose tiles.⁵

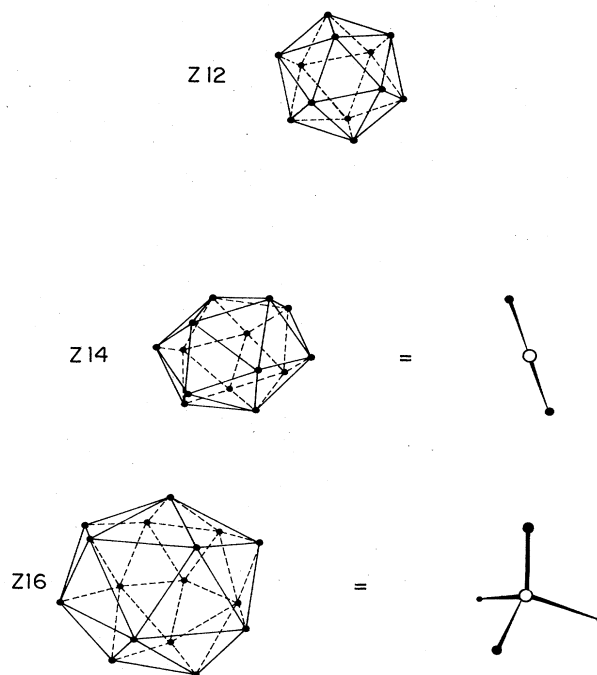


FIG. 4. Three coordination cages which occur in the Mosseri-Sadoc model. Atoms at the centers are not shown. When near-neighbor bonds are assigned via the Voronoi construction, sixfold disclination lines are connected to the central particle in Z14 and Z16.

Figure 5 shows the contours of constant structure factor,

$$S(\mathbf{q}) = \left| \sum_j e^{i\mathbf{q} \cdot \mathbf{r}_j} \right|^2, \quad (6)$$

where the \mathbf{r}_j 's are the positions of a relaxed 197-particle cluster. These particles were taken from the core of a 1549-particle configuration obtained from two iterations applied to the initial icosahedron. Only core atoms were considered to reduce effects due to the boundary. The results were insensitive to the precise group of core atoms we used. The patterns normal to the fivefold and threefold symmetry axes are quite similar to those observed experimentally for $\text{Al}_{0.86}\text{Mn}_{0.14}$.¹ The intensities are different normal to the twofold axis, however. We find that all peak positions are linear combinations of a phenomenological basis set of either (i) 20 reciprocal-lattice vectors pointing to the faces of an icosahedron or (ii) 12 reciprocal-lattice vectors pointing to the vertices of an icosahedron.

There are qualitative differences between these diffraction patterns and those found for three-dimensional Penrose bricks.⁴ The peaks decrease in width with system size, but are slightly broader than could be accounted for by finite-size effects. We cannot be sure that they approach true delta functions as the particle number tends to infinity. The translational order may be short-range, in contrast to Penrose tilings. The orientational order, however, as embodied in a modulated structure factor, appears quite likely to be long range. Pronounced icosahedral modulations in the structure factor appeared even when

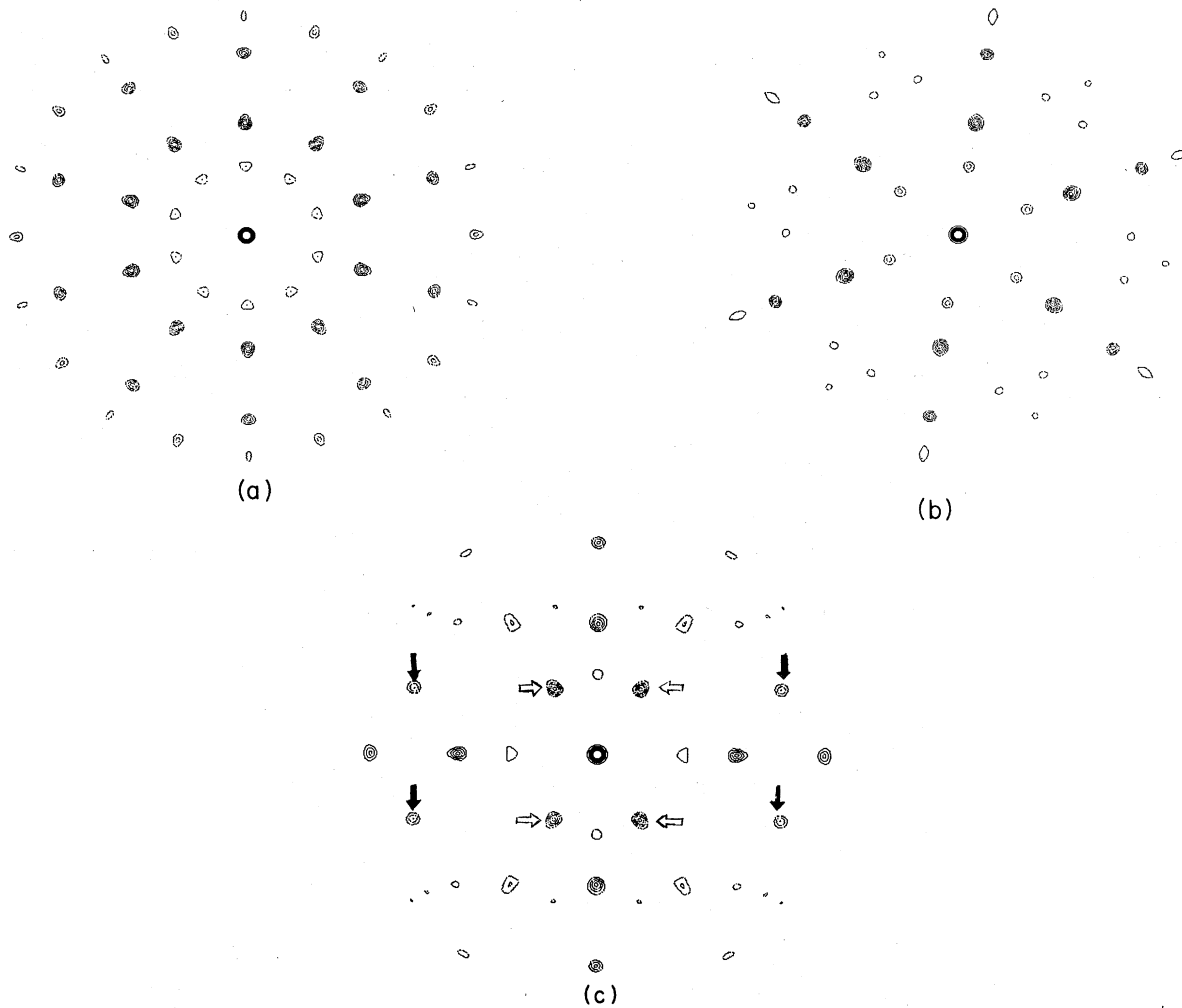


FIG. 5. Contours of constant structure factor normal to the (a) fivefold, (b) threefold, and (c) twofold axes in the Mosseri-Sadoc model, obtained from 197 particles relaxed in a Lennard-Jones pair potential. Full arrows in (c) show the spots which can be used to index all remaining spots via the face model and the open arrows show the spots which index the spots to the vertex model.

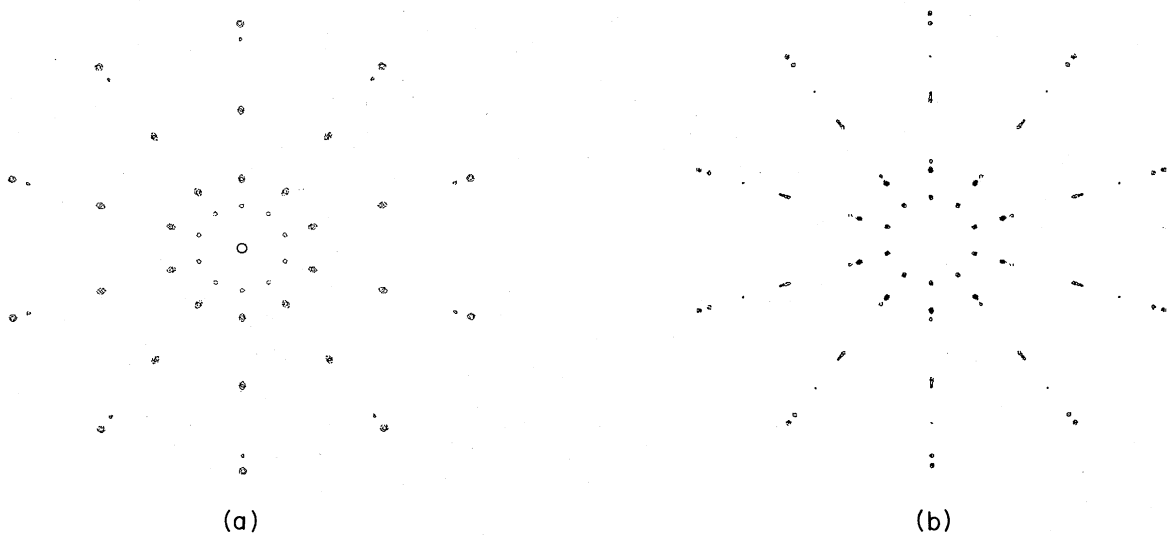


FIG. 6. Structure factor normal to the fivefold axis for relaxed (a) 299- and (b) 933-particle configurations.

we examined configurations of several thousand particles. Although limitations of computer time prevented us from relaxing such large configurations, relaxation produced relatively minor changes in smaller numbers of particles. In large iterates, there was a tendency for the most intense spots to be concentrated along lines of high symmetry in reciprocal space (see the relaxed 299- and 933-particle configurations shown in Fig. 6). This "streaking" appears to be absent in the Penrose patterns.⁴ This effect may be related to "co-lineations" of regularly spaced particles which occur along icosahedral symmetry axes at all length scales. Similar colineations also appear in the Kagome nets which are incorporated into many Frank-Kasper phases.

We close this section with some comments about boundary conditions. As used here, the Mosseri-Sadoc construction could be applied to any initial cluster of tetrahedra. The shape of this cluster determines the macroscopic shape of the limiting particle configuration. The limiting stoichiometry of Z12's, Z14's, and Z16's, however, is determined by Eq. (4), and is independent of the shape. We chose an icosahedral shape because 63% of the particles sit in icosahedral environments. In two dimensions, one could of course apply the construction of Fig. 3(a) to the five distorted triangles which comprise a pentagon, instead of the more natural choice of the six triangles in a regular hexagon. The limiting structure is five regions of hexagonal close-packed lattice separated by five twin boundaries. The boundary conditions lead to a fivefold disclination in the center. The structure factor would be a superposition of the structure factors due to the five differently oriented domains. One might expect similar distortions in three dimensions if, for example, we started with the cluster of 28 tetrahedra comprising a Z16; these boundary conditions force an extra tetrahedral disclination vertex to the center of the particle configuration. It is interesting to note that, even with the icosahedral boundary conditions, the surface of the limiting structure is a highly convoluted, fractal object.

III. DISCUSSION

We have tried to show how Landau theory, already used to model density correlations in conventional crystals,⁶ can be used to describe the icosahedral phases of rapidly cooled metals.¹⁵ Although $\text{Al}_{0.86}\text{Mn}_{0.14}$ is described by the vertex model, it is possible that other materials will be discovered which are edge or face models, just as one finds fcc and bcc, as well as simple cubic crystals in conventional crystallography. The incommensurability of the star of icosahedral reciprocal-lattice vectors leads to peaks everywhere in reciprocal space. There are, in particular, peaks arbitrarily close to the origin, like a conventional crystal in the limit of infinite unit-cell size. This point of view suggests that dislocations in icosahedral phases will be rather usual; because of the infinite unit-cell size all edge dislocation loops may be partial,¹⁶ with a finite stacking-fault energy per unit area in the plane of the loop.

As stressed in Sec. I, the Landau approach is only strictly correct for materials with an infinite translational correlation length, which means resolution limited Bragg

peaks. The other possibility is that these phases are a glassy version of the icosahedral liquid-crystal state proposed in Ref. 2, with a large but finite translational correlation length. If so, there will be a statistical distribution of particle positions in real space, and it would not make sense to attempt absolute structure determinations based on the diffraction pattern in reciprocal space.

In Sec. II, we showed that there are extended icosahedral correlations in a hierarchical Frank-Kasper phase. The construction used here is equivalent to projecting a piece of the curved space Mosseri-Sadoc model into flat space. We were interested in this model because of the predictions of recent order-parameter theories of metallic glasses.¹⁷⁻¹⁹ These theories are more microscopic than the phenomenological Landau approach used here, because they are tied directly to the problems associated with packing tetrahedra of particles in flat space. Networks of -72° disclination lines permeating an icosahedral medium are an inevitable consequence of these theories. These lines can be defined microscopically, via the Voronoi construction,¹³ and should be present in any medium composed of slightly distorted tetrahedra. The Frank-Kasper phases are a particularly simple example.^{12,13} The Shechtman *et al.* experiment shows that icosahedral order can propagate, notwithstanding the presence of these lines. It is interesting to note that the complex crystalline phase of Al_6Mn (which has a 28-atom orthorhombic unit cell²⁰) is closely related to the Frank-Kasper phases, although it contains octahedra as well as distorted tetrahedra.²¹

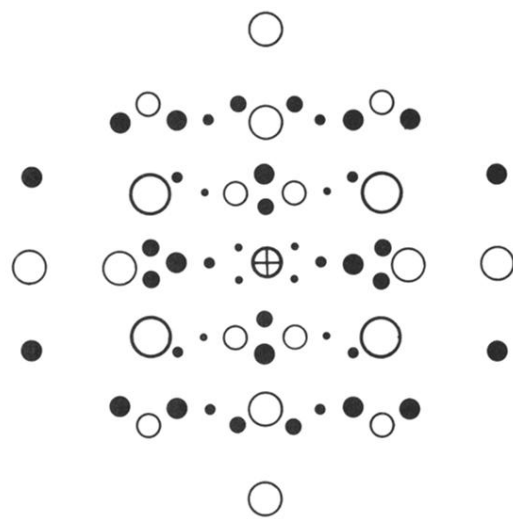
The Mosseri-Sadoc model provides an explicit example of how extended icosahedral order arises in a particular microscopic particle configuration. Although it does not describe $\text{Al}_{0.86}\text{Mn}_{0.14}$ in detail, other alloys, perhaps with $\frac{17}{57} \approx 30$ at. % concentrations of larger atoms occupying Z16 sites, could conceivably form something like a Mosseri-Sadoc phase when cooled rapidly. It would be interesting to use the Voronoi construction to determine the distribution of disclinations in the Penrose models, once one decides what particle configuration to associate with the 3D Penrose bricks.

Note added in proof. After this paper was submitted for publication, we received an interesting paper by Levine *et al.*²² which discusses both Landau theory and a continuum elastic theory of icosahedral Al-Mn. The continuum elastic approach, which is similar to the work by Bak,²¹ is used to show that six-index Burger's vectors are required to describe dislocations in incommensurate icosahedral crystals. None of these dislocations has a purely edge character, consistent with the physical argument given above.

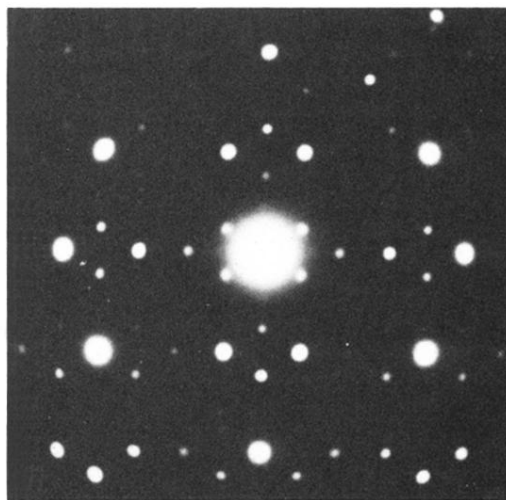
ACKNOWLEDGMENTS

It is a pleasure to acknowledge helpful conversations with B. I. Halperin, P. Horn, K. Kelton, R. Pindak, P. Steinhardt, and M. Widom. We are grateful to P. Bak for a copy of Ref. 15 prior to publication, and to K. Kelton and T. W. Wu for permission to reproduce Fig. 2(b). This work was supported by the National Science Foundation, through the Harvard University Materials Science Laboratory and through Grant No. DMR-82-07431.

- ¹D. S. Shechtman, I. Blech, D. Gratias, and J. W. Cahn, *Phys. Rev. Lett.* **53**, 1951 (1984).
- ²P. J. Steinhardt, D. R. Nelson, and M. Ronchetti, *Phys. Rev. Lett.* **47**, 1297 (1981); *Phys. Rev. B* **28**, 784 (1983).
- ³R. Pindak, D. E. Moncton, S. C. Davey, and J. W. Goodby, *Phys. Rev. Lett.* **46**, 1135 (1981); the compound 95SBC is discussed in J. Budai, S. C. Davey, R. Pindak, and D. E. Moncton, Stanford Synchrotron Radiation Laboratory Report, 1985.
- ⁴D. Levine and P. J. Steinhardt, *Phys. Rev. Lett.* **53**, 2477 (1984).
- ⁵A. L. MacKay, *Physica* **114A**, 609 (1982); P. Kramer and R. Neri, *Acta Crystallogr. Sec. A* **40**, 580 (1984), and references therein. The 3D Penrose tiling constructed by Kramer and Neri is the same as that proposed (independently) by Steinhardt and Levine in Ref. 4.
- ⁶L. D. Landau, *Phys. Z.* **11**, 26 (1937); *The Collected Papers of L. D. Landau*, edited by D. ter Haar (Gordon and Breach—Pergamon, New York, 1965), p. 193; see also G. Baym, H. A. Bethe, G. Baym, and C. Pethick, *Nucl. Phys.* **A175**, 1165 (1971).
- ⁷S. Alexander and J. P. McTague, *Phys. Rev. Lett.* **41**, 702 (1978).
- ⁸N. G. de Bruijn, *Ned. Akad. Weten. Proc. Ser. A* **43**, 39 (1981); **43**, 53 (1981).
- ⁹K. F. Kelton and T. W. Wu, *Appl. Phys. Lett.* **46**, 1059 (1985).
- ¹⁰N. W. Ashcroft and N. D. Mermin, *Solid State Physics* (Holt, Rinehart and Winston, New York, 1976), Chap. 9.
- ¹¹R. Mosseri and J. F. Sadoc, *J. Phys. (Paris) Lett.* **45**, L827 (1984).
- ¹²F. C. Frank and J. S. Kasper, *Acta Crystallogr.* **11**, 184 (1958); **12**, 483 (1959).
- ¹³D. R. Nelson, *Phys. Rev. B* **28**, 5515 (1983), and references therein.
- ¹⁴M. R. Hoare, *Adv. Chem. Phys.* **40**, 49 (1979).
- ¹⁵While this work was in progress, we learned of similar efforts along these lines by P. Bak, *Phys. Rev. Lett.* **54**, 1517 (1984), and unpublished.
- ¹⁶See, e.g., J. Hirth and J. Lothe, *Theory of Dislocations* (McGraw-Hill, New York, 1967).
- ¹⁷J. P. Sethna, *Phys. Rev. Lett.* **50**, 2198 (1983).
- ¹⁸D. R. Nelson and M. Widom, *Nucl. Phys.* **B240** [FS12], 113 (1984).
- ¹⁹S. Sachdev and D. R. Nelson, *Phys. Rev. Lett.* **53**, 1947 (1984); *Phys. Rev. B* (in press).
- ²⁰A. D. I. Nicol, *Acta Crystallogr.* **6**, 285 (1953).
- ²¹W. B. Pearson, *The Crystal Chemistry and Physics of Metals and Alloys* (Wiley, New York, 1972), Chap. 14.
- ²²D. Levine, T. C. Lubensky, S. Ostlund, S. Ramaswamy, P. J. Steinhardt, and J. Toner, *Phys. Rev. Lett.* **54**, 1520 (1985).



(a)



(b)

FIG. 2. (a) First seven generations of spots normal to the twofold axis for the vertex model. (b) Experimental twofold diffraction pattern for $\text{Al}_{0.86}\text{Mn}_{0.14}$ (Ref. 9).